THE ASTROPHYSICAL JOURNAL, 444:458–470, 1995 May 1

A NUMERICAL STUDY OF RESONANT ABSORPTION IN A MAGNETOHYDRODYNAMIC CAVITY DRIVEN BY A BROADBAND SPECTRUM

ANDREW N. WRIGHT AND GRAHAM J. RICKARD
Department of Mathematical and Computational Sciences, University of St Andrews, St Andrews, Fife, Scotland, UK
Received 1994 August 31; accepted 1994 November 7

ABSTRACT

A nonuniform one-dimensional magnetohydrodynamic cavity is driven by a prescribed random boundary motion which has a broadband frequency spectrum. The time-dependent behavior of the system is calculated numerically, and two criteria are identified for the efficient excitation of an Alfvén resonance: (1) The fast, or global, eigenfrequencies of the cavity must lie within the spectrum of the driving motions. (2) The fast eigenfrequencies must lie within the Alfvén continuum. When these conditions are met, a broadband driving motion will excite Alfvén resonances at frequencies corresponding to the fast eigenfrequencies—even though these frequencies may not be particularly favored in the driving spectrum. Our results confirm the importance of the fast global modes noted by previous studies which employed steady harmonic driving. Our principal result is that resonant excitation of Alfvén waves can still occur when a cavity is driven by a nonmonochromatic source, and it gives confidence that resonant coupling may indeed play a key role in heating the solar corona and establishing geomagnetic pulsations—situations in which nature does not provide a monochromatic driving motion.

Subject headings: magnetic fields — MHD — Sun: oscillations — waves

1. INTRODUCTION

The coupling of different magnetohydrodynamic (MHD) wave modes in nonuniform media is a fundamental problem of interest to all plasma physicists. Laboratory plasmas may be heated by resonant interaction between fast (magnetoacoustic) and Alfvén waves (Vaclavik & Appert 1991, and references therein), and it is believed that the same mechanism is responsible for the high temperatures observed in the solar corona (Ionson 1978). The same wave interaction is thought to be at play during the excitation of low-frequency pulsations in the Earth's magnetosphere (Chen & Hasegawa 1974; Southwood 1974), although the heating aspect of the solution is not of primary interest in this context.

Despite the disparte settings mentioned above, the theoretical studies of resonant fast and Alfvén wave coupling demonstrate a coherent investigation of a common problem, regardless of the initial motivation. The driven Alfvén resonance problem of laboratory, magnetosphere, and solar plasma physicists may be regarded as a minor deviant of the following problem: A nonuniform MHD cavity containing field lines (with natural Alfvén frequencies that vary with position) is driven by motion at the cavity boundary. In the case of laboratory experiments the cavity boundary is the surface of a plasma inside a toroidal chamber. This surface is perturbed by currents flowing in an external antenna (Poedts, Goossens, & Kerner 1989a). The magnetospheric cavity is bounded by the magnetopause and may be disturbed by the presence of the Kelvin-Helmholtz instability at the interface (Southwood 1974; Chen & Hasegawa 1974), or by dense clouds in the solar wind striking this boundary (Southwood & Kivelson 1990; Wright 1992a). In the solar problem, the cavity is a coronal loop or arcade whose field lines are fixed in the denser photosphere. Motion of the photospheric plasma due to convection serves as the cavity boundary motion which is the source of wave energy in the cavity.

To some extent, particularly in early investigations, the laboratory, magnetospheric, and solar communities developed their modeling independently. Nowadays there is much "cross-fertilization" of ideas and techniques between the different camps, most notably the adoption of the laboratory studies by the solar community. The efforts of the magnetospheric community are, perhaps, not so well known in general. We shall make a particular effort to cite some of the innovative or key magnetospheric papers in an effort to further the fruitful exchange of ideas on resonant absorption.

Before giving a brief review of the past work, it is necessary to establish some concepts and definitions. The Alfvén frequency $\omega_A(r)$ is the natural frequency that an Alfvén wave on a given field will oscillate at in an undriven system. For an inhomogeneous cavity in which magnetic field and/or density vary, $\omega_A(r)$ will be a function of position—although constant on any given field line. The other important wave mode for our study is the fast (magnetoacoustic) wave. The fast mode, which is somewhat similar to a sound wave in a neutral gas, is not confined to specific field lines but extends throughout the entire cavity. The natural fast-mode waves of a cavity are termed "global" modes, and any cavity may support many of these modes. (The definition of a global mode is given more completely below.)

Sections 1.1 and 1.2 present brief reviews of solar and magnetospheric research, respectively. If the reader is already familiar with this material these sections may be omitted.

1.1. *Solar Studies*

The incompressible and cold (or low-β) plasma approximations are the two limits which have been investigated in most detail by the solar community. The equations governing both these limits were studied previously in different contexts. For example, solar research built on the mathematical similarity between Sedlacek's (1971) study of resonant singularities in electrostatic plasma oscillations and the incompressible MHD equations. Ionson (1978) exploited this similarity in a series of papers and addressed coronal heating by resonant absorption for analytical steady state one-dimensional models.

(By "steady state" we mean all perturbations have a time dependence of $e^{i\omega t}$, where ω is real unless specified otherwise.)

Rae & Roberts (1981) and Lee & Roberts (1986) generalized Ionson's calculations by solving the undriven initial value problem of incompressible ideal MHD. They noted that in the ideal limit there is no heating, but simply a channeling of energy into Alfvén waves. Asymptotically ($t \to \infty$) fine scales develop (phase mixing), so even a small resistivity will ultimately give rise to plasma heating. More recently, Cally (1991) has presented numerical solutions of this initial value problem and his results show the development of increasingly small scales most clearly.

The steadily driven incompressible problem was addressed by Hollweg (1984, 1987), who found that the cavity produced by coronal field structures could act as a resonator and absorb energy from the surrounding medium very efficiently at certain (natural) frequencies. He also confirmed that the decay rate was independent of viscosity or resistivity—thus supporting Ionson's conjecture that the ultimate dissipation rate is simply the ideal decay rate.

Further solar studies moved away from the incompressible limit and considered both warm and cold (low-β) plasmas—e.g., the one-dimensional steady state ($e^{i\omega t}$) calculations of Hollweg (1990) and Sakurai, Goossens, & Hollweg (1990a, b), the latter papers estimating the power that can be absorbed by sunspots and deriving "connection formulae" or "jump conditions" which must be satisfied at the resonant layer. Continuing this line of research, Goossens & Hollweg (1993) calculated the fraction of incident power upon a flux tube/sunspot that could be absorbed and found they were able to tune their model to produce no reflected power. Little effort has been expended in obtaining time-dependent analytical solutions to the undriven initial value problem for these equations (Radoski 1974), perhaps because of increased access to computers nowadays.

Over recent years many numerical solutions to the one-dimensional warm and low-β plasma equations have been calculated, for example, the steady state ($e^{i\omega t}$) calculations of Grossman & Smith (1988), Poedts, Kerner, & Goossens (1989b), and Poedts, Goossens, & Kerner (1990a), and references therein. In particular the latter studies noted that efficient conversion of fast-mode to resonant Alfvén wave energy occurred when ω was close to a fast global mode frequency—a point to which we return later.

Time-dependent numerical solutions to these equations have also been calculated (e.g., Poedts et al. 1990a, b; Steinolfson & Davila 1993). All of these studies drive the MHD cavity with a periodic boundary motion ($e^{i\omega t}$) and study the time-dependent way in which the solution asymptotically approaches the steady state solution. (Most of these numerical studies remove the resonant singularity by introducing a small nonzero resistivity.) These calculations, and in particular Steinolfson & Davila (1993), stress the importance of driving the boundary at a frequency close to a global mode frequency if efficient heating is to be realized.

Of course, coronal magnetic structures are not really one-dimensional. Motivated by laboratory experiments, Goedbloed (1975) considered steady state resonant absorption in two-dimensional equilibria, and this has been continued recently by Poedts & Goossens (1991).

1.2. *Magnetospheric Studies*

The importance of MHD waves for understanding the Earth's magnetosphere was recognized as long ago as 1954 by Dungey (see also Dungey 1967). Magnetospheric studies of fast and Alfvén wave resonant coupling have largely concentrated on the cold (low-β) plasma limit. The first analytical studies of waves in one-dimensional equilibria considered the steady state ($e^{i\omega t}$) solutions (Southwood 1974; Chen & Hasegawa 1974). The governing equations were identical to those that arose in the problem of radio wave propagation in the ionosphere, studied by Budden (1961). The solution has the property of a logarithmic singularity at the field line where $\omega_A^2(x) = \omega^2$. Southwood (1974) and Chen & Hasegawa (1974) suggested that the Alfvén resonance (termed a "magnetic pulsation") could be driven by boundary motions at the magnetopause (the cavity boundary) associated with the Kelvin-Helmholtz instability. The nature of the singularity in Budden's and Sedlacek's equations is identical, and many of the techniques described by Sedlacek (1971) have been employed by modelers in the magnetospheric community.

The heating associated with the currents in the Alfvén waves is not of primary importance to magnetosphericists. To avoid the unphysical singular nature of the solution it is necessary to include some sort of dissipation. In the magnetosphere this is traditionally included by introducing a finite conductivity in the ionospheric boundary, rather than a finite resistivity in the body of the cavity (Kivelson & Southwood 1986; Inhester 1986).

The one-dimensional time-dependent initial value problem was addressed analytically by Radoski (1974). His asymptotic ($t \to \infty$) results show clearly how the initial fast-mode energy is converted into Alfvén wave energy and the solution becomes dominated by phase mixing in an ideal system. Radoski was somewhat ahead of his time and as early as 1976 was performing numerical solutions of the undriven one-dimensional initial value problem. This pioneering study demonstrated the importance of the global mode frequency. Regretably, Radoski (1976) published his results solely as an internal US Air Force report which was not widely available. This work was largely unknown, and it was another decade before the ideas would be advanced independently by other workers.

Observations of magnetic pulsations (Lin et al. 1992) show that several discrete Alfvén resonances are generally excited in the magnetospheric cavity. Although Radoski (1976) had demonstrated this behavior, the idea was advanced independently by Kivelson & Southwood (1985) a decade later. They suggested that an impulsive excitation of the magnetospheric cavity would cause it to oscillate at the natural fast (i.e., global mode) frequencies of the cavity. They argued that on field lines where ω_A is equal to a global mode frequency resonant coupling will produce a particularly large Alfvén wave. They modified the steady state calculations of Budden (1961) and Southwood (1974) to give what is referred to as the cavity model of the magnetosphere (Kivelson & Southwood 1985).

The one-dimensional numerical solutions initiated by Radoski (1976) were continued by, e.g., Allan, Poulter, & White (1986a), Allan, White, & Poulter (1986b), and Inhester (1987), who studied the undriven initial value problem and that of a cavity with an impulsively driven magnetopause boundary. Such calculations confirmed the importance of global modes in determining the frequencies at which resonant excitation would occur.

At this point it is worth defining the term "global mode" more precisely. We have used it somewhat loosely so far to mean a natural fast mode, and indeed this is the sense in which many researchers use the term. The independent development of solutions to the type of equations governing resonant

absorption in many areas of mathematical physics has led to several terms being coined for the same solution. Global modes also go under the names "damped eigenmode," "collective mode," and "quasi mode." Sedlacek (1971) and Zhu & Kivelson (1988) note that, when the real part of the frequency of a fast mode matches ω_A somewhere, there exists the possibility of a solution in which every point in the plasma oscillates with the same *complex* frequency, representing a damped oscillating fast wave. The damping is not due to dissipation in this ideal calculation, but represents the loss of fast-mode energy to the growing Alfvén resonance.

The terms "global" and "collective" seem particularly appropriate to these solutions; when the equations are solved by a Laplace transform involving contour integration in the complex ω-plane it turns out that the position of the poles of the integrand have no dependence on the spatial coordinate (Zhu & Kivelson 1988). Thus, on inverting the Laplace transform, all points in the plasma have the same frequency dependence. Some readers may be concerned that ideal MHD must produce real eigenfrequencies, not complex ones. This is certainly true on the principal Riemann sheet. However, the complex eigenfrequencies corresponding to the global modes do not occur on the principal Riemann sheet, but are located through a branch cut just off the real ω-axis on the next Riemann sheet. There is clearly a mathematical distinction between a fast mode and global mode; a fast mode may be called a global mode if the real part of its frequency matches an Alfvén frequency somewhere (i.e., it lies within the Alfvén continuum), if not it is simply a fast eigenmode and will have a real frequency.

The structure of the equilibrium field in the Earth's magnetosphere is known in far greater detail than those of coronal arcades or loops. Consequently, the magnetospheric community have had considerable motivation to develop resonant coupling models in two-dimensional equilibria. The steady state problem has been addressed by Southwood & Kivelson (1986), Chen & Cowley (1989), Mond, Hameiri, & Hu (1990), and Wright (1991). These studies produce a leading-order singular solution that is still logarithmic. Further calculations by Thompson & Wright (1993) and Wright & Thompson (1994) for the steady state two-dimensional problem are able to recover both the singular and regular solutions. Wright & Thompson (1994) also show how a numerical solution may be matched on the analytical series solution at the resonance (cf. the one-dimensional calculations of Grossman & Smith 1988 and Zhu & Kivelson 1988).

Some recent progress has been made on the two-dimensional time-dependent initial value problem by analytical (Wright 1992a, b) and numerical (Lee & Lysak 1989) methods, confirming the importance of global modes for establishing resonant Alfvén waves in two-dimensional equilibria. Lee & Lysak (1991) also consider a cavity driven with a periodic boundary motion. For a more detailed discussion of magnetospheric studies, see the review by Wright (1994).

1.3. *Time-dependent Forcing*

Having detailed the investigations of resonant wave coupling to date we are in a suitable position to explain how the present calculation extends the existing literature. We investigate the response of an MHD cavity to a nonperiodic driven boundary motion. Such a broadband source may approximate the photospheric motions that excite waves in coronal structures, or the unpredictable buffeting of the magnetospheric cavity by the solar wind. Mathematically, we idealize the cavity to a one-dimensional equilibrium [uniform magnetic field and $\rho(x)$] and neglect plasma pressure. The displacement of one end of the cavity is then varied randomly, and the governing equations are solved numerically in (x, t)-space.

Existing time-dependent numerical solutions all solve for either (1) an impulsive driver (and subsequent undriven boundary conditions) or (2) a periodically driven boundary condition. Both types of experiment can produce localized Alfvén resonances. In case 1, the problem is essentially an initial value problem following the short impulsive phase. The disturbance may be thought of as a sum over the natural fast modes of the cavity, and field lines where ω_A matches a fast eigenfrequency may experience the growth of a resonant Alfvén wave (Kivelson & Southwood 1985). In case 2, the system is being forced with a single frequency, and not surprisingly a resonant Alfvén wave is excited on field lines where ω_A matches the driver frequency (Poedts et al. 1990a, b). Indeed, Poedts et al. (1990b) find Alfvén wave excitation at a global mode frequency also during the transient phase. However, as $t \to \infty$ only Alfvén waves of the driving frequency survive.

To the best of our knowledge the present results are the first time an MHD cavity has been examined with a random broadband driven boundary motion. If a plasma is to be heated efficiently through ohmic dissipation it is necessary to generate large current densities—such as at a resonance. It is not clear that a broadband driver will generate this feature.

It may be argued that, if the time-dependent solution is calculated for a series of periodically driven boundary conditions ($e^{i\omega t}$), then the solution arising from a more general temporal boundary condition may be synthesized by taking an appropriate Fourier sum (cf. Grossman & Smith 1988). While this is certainly true of the linear wave fields, it is not obvious that the quadratic energies of the periodic solutions (when summed) have any physical meaning. Indeed, it is not immediately obvious whether a solution constructed by such a Fourier integral approach will contain the fine-scale structure required for laboratory and coronal heating. If it does, are the small scales distributed evenly throughout the cavity, or concentrated in a "resonance"? In a magnetospheric context, we do not know whether to expect discrete magnetic pulsations to be excited by a broadband source. It is in an effort to answer these questions, and understand the physical mechanisms which operate in MHD cavities, that the present work is presented.

The paper is structured as follows: § 2 considers the coupling of boundary motions to the fast mode in a (uniform) cavity. In § 3 we speculate about the excitation of the fast mode in a nonuniform cavity, and how it may couple to Alfvén resonances. We identify two criteria for the efficient excitation of Alfvén waves in a cavity driven by a broadband source. Section 4 presents numerical simulations of an MHD cavity driven by a broadband source. Section 5 discusses the results, and § 6 summarizes our main points.

In keeping with the underlying unity of resonant absorption studies in all areas of plasma physics we do not direct our paper or results at any single application, preferring to address the fundamental physics operating in these systems. (In § 5 we discuss briefly the implications of our work for magnetospheric and solar physics.)

2. FAST MODE DRIVEN BY BOUNDARY MOTIONS

Consider a low-β plasma of density $\rho(\boldsymbol{r})$ with uniform resistivity η permeated by a uniform magnetic field $\boldsymbol{B} = B\hat{\boldsymbol{z}}$. The

MHD equations governing the linear velocity ($\boldsymbol{u}$) and magnetic field ($\boldsymbol{b}$) perturbations are

$$\frac{\partial u_x}{\partial t} = \frac{V^2}{B}\left(\frac{\partial b_x}{\partial z} - \frac{\partial b_z}{\partial x}\right), \tag{1a}$$

$$\frac{\partial u_y}{\partial t} = \frac{V^2}{B}\left(\frac{\partial b_y}{\partial z} - \frac{\partial b_z}{\partial y}\right), \tag{1b}$$

$$\frac{\partial b_x}{\partial t} = B\frac{\partial u_x}{\partial z} + \frac{\eta}{\mu_0}\nabla^2 b_x, \tag{1c}$$

$$\frac{\partial b_y}{\partial t} = B\frac{\partial u_y}{\partial z} + \frac{\eta}{\mu_0}\nabla^2 b_y, \tag{1d}$$

$$\frac{\partial b_z}{\partial t} = -B\left(\frac{\partial u_x}{\partial x} + \frac{\partial u_y}{\partial y}\right) + \frac{\eta}{\mu_0}\nabla^2 b_z, \tag{1e}$$

where $V^2 = B^2/\mu_0\rho$ is the Alfvén speed squared. Note that we have not allowed for the fact that the plasma will be heated by ohmic dissipation—we shall either consider the ideal limit ($\eta \to 0$), or assume that heat is radiated/conducted away on a short timescale compared to MHD wave periods so that the low-β equations above are a good approximation.

Throughout this paper we shall assume that the field lines are line-tied in the z-direction and consider solutions that are standing in z with wave number k_z, and periodic in y with wave number k_y.

We begin by considering normal-mode solutions to the equations (1) in a uniform density cavity and assume all variables have a time dependence of $e^{i\omega t}$. The governing equations may be reduced to

$$\frac{d^2u_x}{dx^2} + \left(\frac{\omega^2}{V^2} - k_y^2 - k_z^2\right)u_x = 0. \tag{2}$$

The general solution to equation (2) has the form

$$u_x(x) = A_1 \sin(k_x x) + A_2 \cos(k_x x), \tag{3}$$

where

$$k_x^2(\omega) = \frac{\omega^2}{V^2} - k_y^2 - k_z^2 \tag{4}$$

and A_1 and A_2 are constants.

Suppose that there are perfectly reflecting boundaries at $x = 0$ and x_0, e.g.,

$$u_x(0) = 0, \quad u_x(x_0) = 0, \tag{5}$$

then the solution to equations (3) and (4) requires $A_2 = 0$ and $k_x = n\pi/x_0$. Thus the natural eigenfrequencies of an undriven cavity are

$$\omega_n^2 = V^2\left(\frac{n^2\pi^2}{x_0^2} + k_y^2 + k_z^2\right). \tag{6}$$

Now let us focus on the solution when the boundary at $x = 0$ moves periodically. Clearly this is an important aspect of the resonance problem since energy will arrive at the resonant field lines in the form of a fast wave (unless the footpoints of a field line are disturbed). Assuming the velocity at $x = 0$ to vary as $u_0 e^{i\omega t}$, the boundary conditions become (suppressing the $e^{i\omega t}$ dependence common to all perturbations)

$$u_x(0) = u_0, \quad u_x(x_0) = 0. \tag{7}$$

The boundary condition at $x = 0$ is rather like a piston in hydrodynamics. We assume that $u_x(0)$ has this form regardless of any waves that may be incident upon it from within the cavity—such waves will simply be reflected. This description is reasonable if the energy density of the "piston" motion is much greater than the energy density of the MHD cavity waves (cf. large photospheric or magnetosheath kinetic energy densities relative to the magnetic energy density). We note that boundary motions at $x = 0$ are not the ideal way to simulate photospheric driving, which would move the boundaries at the ends of the field lines. However, the present method (besides being appropriate for a magnetosphere driven by magnetopause motions) has the merit of requiring explicit solution in only one spatial coordinate. For this reason many previous solar studies have employed a similar "side boundary" type of driving (e.g., Poedts et al. 1990a; Steinolfson & Davila 1993).

Employing equation (7) to determine the constants A_1 and A_2, we find the solution for $u_x(x, t) = u_x(x)e^{i\omega t}$,

$$u_x(x) = u_0\left[\cos(k_x x) - \frac{\cos(k_x x_0)}{\sin(k_x x_0)}\sin(k_x x)\right], \tag{8}$$

where $k_x(\omega)$ is given in equation (4).

Evidently the amplitude of u_x becomes large whenever

$$k_x x_0 \approx n\pi \quad (\text{i.e., } \omega^2 \approx \omega_n^2), \tag{9}$$

equivalent to requiring that the frequency of the boundary motion be close to a natural (fast or global) mode frequency of the cavity. This behavior is demonstrated in Figure 1, which plots $|u_x|$ at $x = 0.3x_0$ as a function of ω when $k_y = k_z = \pi/x_0$. The result is not surprising; however, it is important to establish this property clearly for interpreting later solutions.

If we are to couple boundary motions to Alfvén waves, the information must reach these field lines via a fast mode. Moreover, if we require a large conversion of fast-mode energy to Alfvén energy, then we will require a correspondingly large-amplitude fast mode to exist.

Some studies calculate the "fractional absorption" (f_A) as a function of frequency (Grossmann & Smith 1988; Poedts et al. 1989a; Steinolfson & Davila 1993), representing, essentially, the rate of increase of resonant Alfvén energy for a unit amplitude driver. These studies find f_A has a peak when the driving frequency matches a global mode frequency. Although no explanation for this result has been offered, we suggest that it is

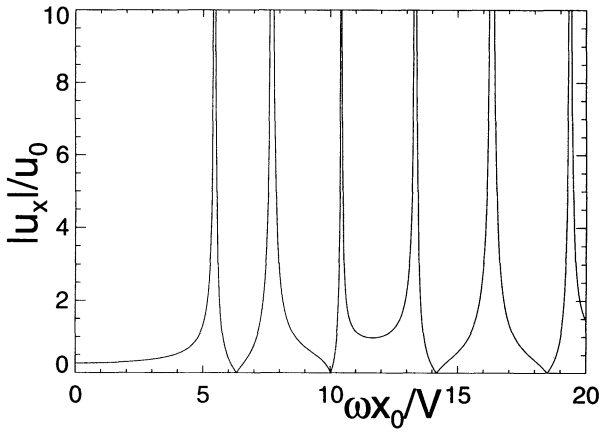

FIG. 1.—Amplitude of the x-component of velocity in a uniform MHD cavity driven by a boundary motion $u_x(0, t) = u_0 e^{i\omega t}$. The peaks occur at frequencies equal to a natural fast eigenfrequency of the undriven cavity.

a result of a relatively large amlitude fast mode being excited when the driver and global frequencies are matched, which in turn drives a relatively large Alfvén wave. Thus we arrive at our first criterion for efficient resonant excitation of Alfvén waves: *the global (or fast) mode eigenfrequencies of the cavity must lie within the frequency spectrum of the driving motions.*

3. EXCITING RESONANT ALFVÉN WAVES

Resonant excitation of Alfvén waves may occur when the cavity is inhomogeneous. It is sufficient to let the density vary in the x-direction, $\rho(x)$. The ideal form of equations (1) may now be written in terms of $u_x(x)$:

$$\frac{d^2u_x}{dx^2} - \frac{k_y^2}{\omega^2/V^2 - k_z^2}\left[\frac{d}{dx}\ln\left(\frac{\omega^2}{V^2} - k_y^2 - k_z^2\right)\right]\frac{du_x}{dx} + \left(\frac{\omega^2}{V^2} - k_y^2 - k_z^2\right)u_x = 0 , \quad (10)$$

which contains a singularity at x_r, where

$$\omega_A^2(x_r) \equiv k_z^2 V^2(x_r) = \omega^2 . \quad (11)$$

This position is where the local Alfvén frequency (defined above) matches the driving frequency. It is well known that in the ideal calculation ($\eta = 0$) b_x, $u_x \approx \ln|x - x_r|$ and b_y, $u_y \approx 1/(x - x_r)$, while b_z is regular at x_r (Southwood 1974). If some dissipation is included in the form of resistivity, then the singularity is resolved into a finite-size region centered on x_r whose width varies as $\eta^{1/3}$.

The perturbed quantities u_x, b_x, and b_z (away from x_r) are associated with the fast mode, whereas b_y and u_y (particularly when near x_r) are predominantly Alfvénic perturbations.

Another characteristic position in the solution to equation (10) is found from WKB theory. The fast mode is able to propagate into higher and higher Alfvén speed regions until $x = x_t$ (the turning point, defined below) beyond which it is evanescent (Southwood 1974):

$$\omega^2 = (k_y^2 + k_z^2)V^2(x_t) . \quad (12)$$

Evidently the position of the resonance is always located in the evanescent tail of the fast mode. (From eqs. (4) and (11), $k_x(\omega, x_r)$ is always imaginary.)

The coupling strength between fast and Alfvén waves depends upon the equilibrium and wavenumbers (Budden 1961; Kivelson & Southwood 1986). In particular, the coupling is weak when $k_y = 0$, or $k_y \to \infty$. However, if the fast wave (u_x) is to drive an Alfvén resonance, it is necessary that somewhere in the cavity equation (11) be satisfied; i.e., *the frequency of the fast mode must lie within the Alfvén continuum.* This is our second criterion for the efficient excitation of (or heating by) Alfvén waves.

What is the fate of the fast eigenfrequencies (eq. [6]) in a nonuniform cavity? Suppose the region $0 < x < x_t$ corresponds to the propagating region; then the WKB estimate of the nth eigenfrequency ω_n is

$$\int_0^{x_t} \sqrt{\frac{\omega_n^2}{V^2} - k_y^2 - k_z^2}\, dx = (n + \alpha)\pi , \quad n = 1, 2, 3, \ldots , \quad (13)$$

the phase factor α being determined by the boundary conditions in x (Inhester 1987). Alternatively, equation (10) may be solved numerically to find ω_n (Zhu & Kivelson 1988). Whichever method is employed, the important feature is that natural fast or global modes still persist in a nonuniform cavity, and consequently, we would expect the qualitative behavior of Figure 1 to be representative of nonuniform cavities.

We noted previously that it is possible to sum many linear solutions in an effort to generate a more general time-dependent solution. Figure 1 suggests that such a sum will weight the solutions with $\omega \approx \omega_n$ very heavily—and it seems likely that these "global mode" resonances will dominate the solution. This conjecture is tested by our numerical calculations.

A discussion of the energetics of a "summed" solution is appropriate only when the summed fields are inserted into the energy equation. It is not physically meaningful to sum individual energy equations; to identify this summed energy as the energy equation of the summed wave fields is misleading (cf. Grossman & Smith 1988; Poedts et al. 1990a).

It is somewhat difficult to anticipate the final summed solution—especially when we take the limit of the sum becoming an integral. For example, an ideal solution of frequency ω has a logarithmic singularity at x_r defined in equation (11). When we sum a continuous range (i.e., do an integral) of such frequency-dependent solutions, do all the logarithmic singularities persist or cancel out?

The questions raised above have motivated us to perform a numerical solution to the one-dimensional time-dependent equations when one boundary is driven by a random broadband displacement. The results are reported in the next section.

4. CHARACTERISTIC FREQUENCIES

The numerical results reported later in this paper are calculated for an MHD cavity similar to that employed by Steinolfson & Davila (1993). The density has the following explicit variation with x:

$$\rho(x) = \rho_0[0.1 + 0.9 \exp(-x^4)] . \quad (14)$$

The cavity extends over the range $0 < x < 3$, and Steinolfson & Davila (1993) argue that this may represent half of a coronal loop when driven from the $x = 0$ boundary. This cavity could also represent the Earth's magnetosphere, the $x = 0$ boundary being the magnetopause. Employing the normalized space dimension implicit in equation (14) and the values of B and ρ at $x = 0$, the remaining physical quantities may also be normalized. Figure 2 shows the variation of the normalized Alfvén speed.

To proceed further we must specify some boundary conditions. In the succeeding sections we shall drive the cavity, but

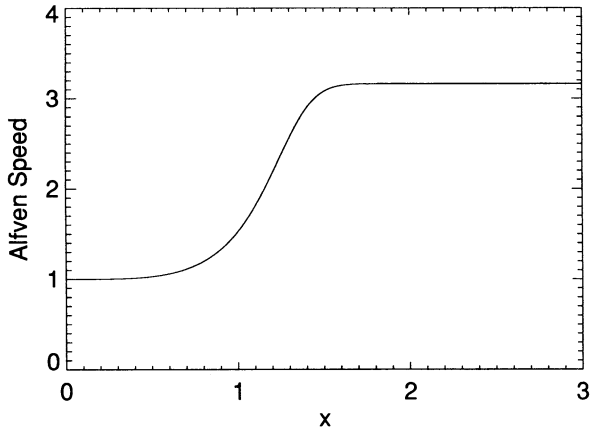

FIG. 2.—Variation of Alfvén speed with x for the model cavity employed in the numerical calculations (see eq. [14]).

for the moment we focus upon the properties of the undriven cavity in an effort to provide a framework for interpreting later results. Steinolfson & Davila (1993) assumed that all perturbations at the boundary $x = 3$ decay as exp $[-(k_y^2 + k_z^2)^{1/2}]$, which is appropriate when $\omega^2/V_A^2(x = 3) \ll k_y^2, k_z^2$, i.e., when $V_A(x = 3)$ becomes very large. However, since $V_A(3)/V_A(0) \approx 3$, this limit is not met very well, and it is not clear what physical interpretation may be placed upon this boundary condition. We prefer to impose simple reflecting boundary conditions,

$$u_x(x = 0) = 0 \quad \text{and} \quad \frac{\partial u_x(x = 3)}{\partial x} = 0 , \tag{15}$$

the latter being chosen because the plasma inertia at $x = 3$ is relatively low. Our outer boundary will trap all energy within the cavity and is likely to give us an upper estimate for the efficiency with which fast-mode energy may be coupled to Alfvén waves (because the fast mode is not able to escape to $x = \infty$). However, we are not likely to seriously overestimate this efficiency because any component of the fast mode which drives a resonance will also have a turning point $x_t < x_r$, and so is effectively trapped and insensitive to any boundary condition at $x = 3$.

The Alfvén continuum and the fast eigenfrequencies depend upon the wavenumbers k_y and/or k_z. We adopt a small wavenumber k_y of 0.1 in order to facilitate comparison with the results of Steinolfson & Davila (1993). Although this value of k_y may not be particularly appropriate to the coronal situation, it is very convenient for our theoretical investigation of the general nature of time-dependent resonant coupling: Fast eigenfrequencies may be estimated from WKB theory (eq. [13]) or (in view of the small value of k_y) from shooting for the eigenfrequencies of equation (10) when k_y is set to zero. (The latter method relies on the fact that $\partial\omega_n/\partial k_y \approx 0$ for small k_y and is the procedure adopted here. The eigenfrequency estimates are reliable to better than 1%; cf. Zhu & Kivelson 1988.) The optimum coupling rate probably occurs for some value of k_y larger than 0.1, and we could scan k_y to determine the exact value. However, as the present paper is concerned with establishing criteria for when relatively efficient coupling takes place we employ $k_y = 0.1$ throughout the remainder of the paper. Future studies may adjust k_y to truly optimize coupling, but for the purposes of the new concepts we wish to establish in this paper a constant value of k_y is quite adequate.

We leave k_z as a free parameter, and by searching in k_z parameter space we may "tune" our cavity to have 0, 1, 2, etc., resonances and may also adjust the frequencies. This will provide an elegant way of examining the two criteria we have identified for efficient resonant absorption. The upper and lower limits of the Alfvén continuum are given by

$$\begin{aligned} \omega_A(x = 0, k_z) &= k_z V_A(x = 0) , \\ \omega_A(x = 3, k_z) &= k_z V_A(x = 3) . \end{aligned} \tag{16}$$

Figure 3 shows the variation of the limits of the Alfvén continuum (*dashed lines*) with k_z. The solid lines are the variation of the fast (global) eigenfrequencies for the first five harmonics. When $k_z \lesssim 0.6$ no fast eigenfrequencies lie within the Alfvén continuum; for $0.6 \lesssim k_z \lesssim 1.6$ the first fast eigenfrequency lies in the continuum; when $1.6 \lesssim k_z \lesssim 2.6$ the first two fast eigenfrequencies lie in the Alfvén continuum, etc. Based upon our second criterion for efficient coupling established in § 3, we anticipate that Figure 3 will play a central role in understanding our results.

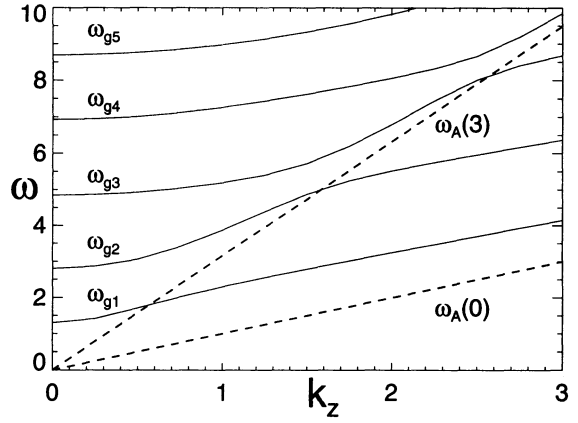

FIG. 3.—Variation of the upper and lower limits of the Alfvén continuum [$\omega_A(0)$ and $\omega_A(3)$] and the first five global fast eigenfrequencies (ω_{gn}, $n = 1, 2, \ldots, 5$) with k_z.

If we assume, for the moment, that the global fast modes do in fact drive Alfvén resonances at the fast eigenfrequencies, then we can calculate the location of the resonance quite simply: For a given k_z Figure 3 yields the fast eigenfrequencies, which together with equations (14) and (11) can be used to evaluate x_{rn}—the position of the resonance driven by the nth fast harmonic. This procedure was repeated over a range of k_z to produce Figure 4. The presence of 1, 2, or more resonances for different values of k_z is again apparent.

5. NUMERICAL RESULTS

In this section we present the numerical results of the cavity described in § 4 when a random, broadband frequency driving term is included. The numerical scheme used to solve the equations is the leapfrog-trapezoidal algorithm of Zalesak (1979) and is second-order accurate in both space and time. The size of the space and time steps is dependent upon the choice of resistivity which limits the spatial scales which can be realized. When the governing equations (1) are cast in dimensionless form [length scale a, velocity $V_A(0)$, etc.], the resistivity is normalized by $\mu_0 V_A(0)a$. We present results with values of dimensionless resistivity (equivalent to the reciprocal of the Lundquist number) equal to 10^{-4} and 10^{-6}. When $\eta = 10^{-4}$ and 10^{-6} the grid spacing is taken as 6×10^{-3} and 2×10^{-3},

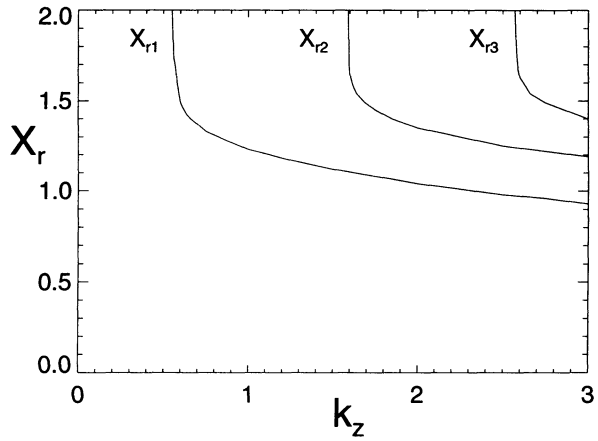

FIG. 4.—Dependence of the location of the Alfvén resonance on k_z: x_{rn} is the position where $\omega_A(x_{rn})$ is equal to the nth fast eigenfrequency, ω_{gn}.

respectively. The time step was chosen to be a fraction (between 0.05 and 0.1) of the minimum propagation or diffusion time across a grid cell. The convergence of our scheme was tested, and continuity of energy was met to typically 1 part in 10^6.

5.1. *Boundary Conditions*

The boundary condition of $\partial u_x/\partial x = 0$ at $x = 3$ is implemented simply as a symmetry condition. The boundary at $x = 0$ is driven by specifying its displacement as a function of time. For the purposes of the present study we want a boundary motion that does not contain a dominant driving frequency, unlike most previous investigations. We devised the following method for producing a broadband driving frequency spectrum. The method relies upon generating a random set of data (ξ_{xn}, t_n) for the x-displacement of the boundary at $x = 0$ at given times, t_n. The data sequence is then fitted with a cubic spline to provide a piecewise continuous expression of $\xi_x(x = 0, t)$ [the velocity $u_x(x = 0, t)$ of the driver may then be obtained by differentiation of the spline function].

In order to avoid transients at $t = t_0 = 0$, when our experiment begins we impose $\xi_{x0} = 0$ and $u_{x0} = 0$. [This was achieved by creating a symmetrical set of data points $(\xi_{x-n}, t_{-n}) = (\xi_{xn}, -t_n)$, $n > 0$, before fitting the spline curve.] Before generating the data points two time intervals are specified, Δt_1 and Δt_2 ($\Delta t_1 < \Delta t_2$). The algorithm is as follows: (1) A random number generator produces a value for ξ_{xn} in the range -1 to $+1$. (2) The time t_n is determined by $t_n = t_{n-1} + \Delta t$, Δt being chosen as Δt_1 with a probability of 90% and Δt_2 with a probability of 10% based upon the output of a second random number generator. (3) Steps 1 and 2 are then repeated until t_n exceeds the time we wish to solve over. (4) One proviso is that, following a choice of the long time step (Δt_2), the next two time steps must be Δt_1 then a random choice is made. Condition 4 was introduced because the long time step Δt_2 leaves the cavity effectively undriven, and two such steps in close succession allow perturbations to decay significantly with the large resistivities employed in our numerical calculations.

The method described above produces a displacement $\xi_x(x = 0, t)$ that moves in a random fashion between -1 and $+1$. The time derivative of the displacement is the velocity at $x = 0$, which may be used to drive the system of equations (1). Given the velocity and field perturbations over the grid at one time, the state after the next time step may be found from updating $\boldsymbol{u}$ and $\boldsymbol{b}$ with equations (1) over the entire grid, except for u_x at $x = 0$ (which is given by the boundary condition algorithm). Of course, equation (1a) actually predicts the acceleration of the plasma at $x = 0$, and this is in general different from the conditions imposed. The mismatch between the two represent an inhomogeneous or driving term that launches waves into the cavity. Centered derivatives are used for calculating $\partial/\partial x$ and $\partial^2/\partial x^2$ except for cells at the $x = 0$ boundary, where one-sided derivatives are employed.

For the results presented here $\Delta t_1 = 1.25$ and $\Delta t_2 = 12.5$. Figure 5*a* shows the driving condition $u_x(0, t)$ and Figure 5*b* shows the Fourier transform. The spectrum has the features we require; a broad frequency range with no single frequency dominating the spectrum.

5.2. *Cavity Response*

To examine the behavior of waves in a driven cavity, we present detailed solutions and energy diagnostics for a case study where $k_z = 1.23$ (the results of this run are shown in Figs. 6–9). When the cavity is driven with the velocity in Figure 5*a* waves are excited in the cavity. Figure 6*a* shows the velocity at a point within the cavity ($x = 2$) as a function of time. It is evident that this velocity has a more coherent oscillatory nature than the driving velocity in Figure 5*a* and is readily verified by taking the Fourier transform of the signal (see Fig. 6*b*). The presence of preferred frequencies is evident. Moreover, the fast or global mode eigenfrequencies for $k_z = 1.23$ are 2.54, 4.35, 5.38, 7.41, and 9.11 (e.g., from Fig. 3) and are shown by dashed lines in Figure 6*b*—these correspond exactly to the locations of the peaks. (Note that we have actually plotted the square root of the Fourier transform in Fig. 6*b* in an effort to make the high-frequency peaks clearer.)

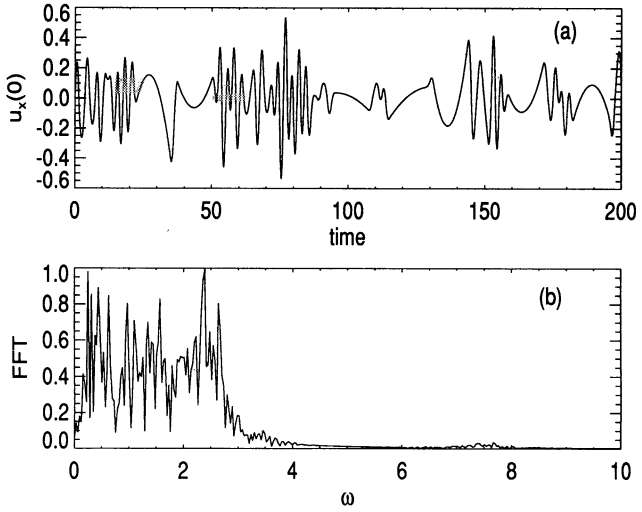

FIG. 5.—(*a*) Random $\hat{x}$ velocity of the driven boundary at $x = 0$ as a function of time. (*b*) Normalized frequency spectrum (FFT) of the driving signal in (*a*).

For small k_y the fast mode comprises essentially perturbations u_x, b_x, and b_z, thus Figure 6 represents basically the amplitude of the fast-mode waves in the cavity. We see that the cavity acts as a filter of the driving spectrum and suppresses frequencies that are not natural frequencies of the cavity. Com-

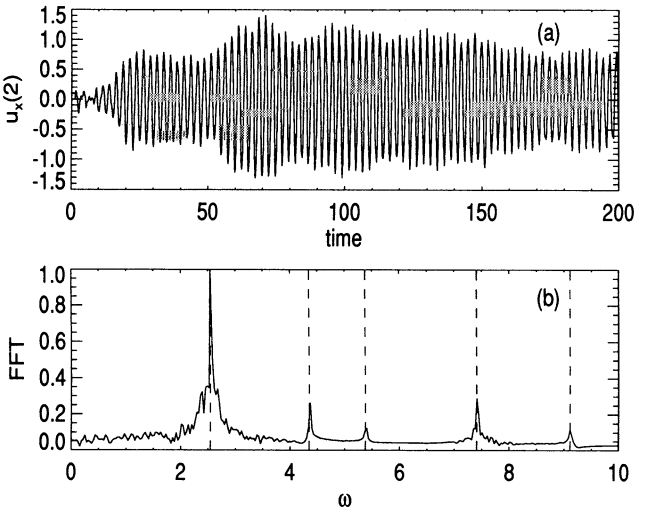

FIG. 6.—(*a*) $\hat{x}$ component of the velocity measured at a point within the cavity ($x = 2$). (*b*) Normalized FFT of the signal in (*a*)—we have actually plotted the square root of the FFT to make the high-frequency peaks clearer. The dashed vertical lines mark the values of global fast eigenfrequencies.

paring with Figure 1, it appears that a nonuniform cavity behaves in a similar fashion to a uniform cavity in this respect.

Consider the relative amplitudes of the peaks in Figure 6*b*: The largest (at $\omega \approx 2.54$) occurs at a position in the driving spectrum (Fig. 5*b*) which has a significant amplitude—thus this mode is driven strongly. The peaks of the harmonics at higher frequencies ($\omega \approx 4.25$ and higher) map to the low-amplitude tail of the driving spectrum (Fig. 5*b*)—thus these modes are driven weakly. (We specifically turned our cavity, by choosing k_z, to demonstrate this behavior.) This explanation agrees well with our results and supports our first criterion for efficient coupling of boundary motion to field line resonances: *Some global/fast eigenfrequencies must lie within the frequency spectrum of the driving motions.*

Note that even when the cavity is effectively undriven ($25 < t < 50$ and $95 < t < 130$) the fast mode within the cavity $u_x(2, t)$ remains oscillatory. Energy is stored within the cavity and provides a constant reservoir during the random injections of energy from the boundary. In fact, the fast-mode wave in Figure 6 is so coherent (monochromatic) that we would expect it to be an excellent driver of Alfvén resonances provided its eigenfrequency lies within the Alfvén continuum.

5.3. *Energy Densities*

The energy total density of our system (E_T) may be expressed (in normalized units) as

$$E_T = \tfrac{1}{2}\rho(u_x^2 + u_y^2) + \tfrac{1}{2}(b_x^2 + b_y^2 + b_z^2)\,. \tag{17}$$

In the limit $k_y = 0$ the fast and Alfvén waves decouple, and we may define the energy densities associated with the fast (E_f) and Alfvén (E_A) waves separately:

$$E_A = \tfrac{1}{2}(\rho u_y^2 + b_y^2)\,, \tag{18a}$$

$$E_f = \tfrac{1}{2}(\rho u_x^2 + b_x^2 + b_z^2)\,. \tag{18b}$$

If $k_y \neq 0$ pure fast or Alfvén solutions do not exist, but are replaced by coupled wave solutions. Nonetheless, the partition of energies in equations (18) remains a surprisingly good method for classifying the dominant character of disturbances unless k_y is particularly large (Rickard & Wright 1994).

Figure 7*a* shows the energy densities E_A and E_f at $t = 200$ for $\eta = 10^{-4}$. The fast-mode energy extends across the entire cavity, being evanescent at large x (large V_A). The Alfvénic energy density (E_A) is confined to a small range $1.1 < x < 1.25$, which may be understood by considering the frequency of the global/fast mode which drives the resonance: the fundamental fast eigenfrequency is 2.54 and is equal to the natural Alfvénic frequency of field lines at $x_r \approx 1.18$ (see Fig. 4). Thus it appears that the broadband frequency boundary motions in Figure 5 can indeed drive a localized resonance if the fast eigenfrequency lies within the Alfvén continuum—our second criterion. This result is of paramount importance to resonant absorption models of coronal heating and is the principal result of our paper.

Figure 7*b* presents the same information as Figure 7*a* but is taken from a run where $\eta = 10^{-6}$. The distribution of E_f is almost identical to that in Figure 7*a*—a property we emphasize by plotting E_f for $\eta = 10^{-6}$ as the dashed line in Figure 7*a*. The minimal change in E_f while η changes by two orders of magnitude suggests that the structure of the fast mode is independent of η, as one would expect. In contrast the Alfvénic energy density changes radically with η. Estimating the

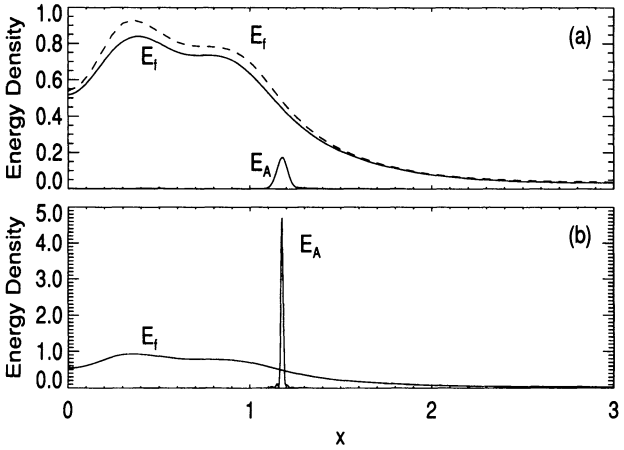

FIG. 7.—(*a*) Spatial variation of the fast and Alfvén energy densities (E_f and E_A) at $t = 200$ when $\eta = 10^{-4}$. (*b*) Same as (*a*), but for $\eta = 10^{-6}$. Note how the E_A peak becomes narrower and taller as η decreases, while the distribution of E_f is hardly changed—a property demonstrated by plotting E_f for $\eta = 10^{-6}$ as the dashed line in (*a*).

FWHM of E_A, from enlargements of these figures, we find that the energy density narrows by a factor of 4–5 when η changes from 10^{-4} to 10^{-6}. Such a change is in surprisingly good agreement with the steady state ($e^{i\omega t}$) analysis which suggest the width should scale as $\eta^{1/3}$—a reduction by a factor of 4.6. The peak of E_A increases as η decreases, being a factor of 26 times larger in Figure 7*b* compared with Figure 7*a*. (Steady state theory predicts $E_A \propto \eta^{-2/3}$, giving a scaling of 22.)

5.4. *Ohmic Heating*

The ohmic dissipation in the plasma (ηj^2) provides an estimate of the heating rates that may be achieved in the corona and can give a measure of the coupling strength between fast and Alfvén waves. Figures 8*a*–8*c* show the spatial variation of the time-integrated ($0 < t < 200$) ohmic dissipation for each of the current components when $\eta = 10^{-4}$ [i.e., $O_x = \int \eta j_x^2\,(x, t)dt$, etc]. The field-aligned current heating (ηj_z^2) is clearly associated with Alfvén waves (cf. Fig. 7*a*), as one would expect; $j_z \approx \partial b_y/\partial x$, and Alfvén waves have a large b_y. It is apparent from the top panel that there is some j_x current and heating associated with the Alfvén resonance, although it is much smaller than j_z. At the resonance $j_x \approx -k_z b_y$, and $\nabla \cdot \boldsymbol{j} = 0$ is met largely by the field-aligned current being directed in the x-direction. (There is no significant j_y current at the resonance.) Note that the j_x heating also shows some evidence of currents associated with the fast mode in the range $0 < x < 0.9$; $j_x \approx k_y b_z$. Heating from j_y currents (O_y; in Fig. 8*b*) arise from the fast mode ($j_y = k_z b_x - \partial b_z/\partial x$).

Figures 8*d*–8*f* display the same quantities as in Figures 8*a*–8*c*, but for a run when $\eta = 10^{-6}$. Note how the form of the j_y heating (O_y) is unchanged. This is to be expected since j_y is associated with the fast mode, whose structure does not depend upon η (see Fig. 7*a*). The magnitude of the j_y heating has been reduced by a factor of 96, showing an approximate scaling with η. The fast-mode j_x heating has been reduced by a similar amount and is not visible in Figure 8*d*. The Alfvénic j_x current heating has been narrowed, in line with expectations from Figure 7, and reduced in magnitude by a factor of ~ 5. Steady linear theory would suggest $j_x \propto j_z \Delta x \propto b_y$ from $\nabla \cdot \boldsymbol{j} = 0$. Since the resonance width $\Delta x \propto \eta^{1/3}$ and $b_y \propto \eta^{-1/3}$,

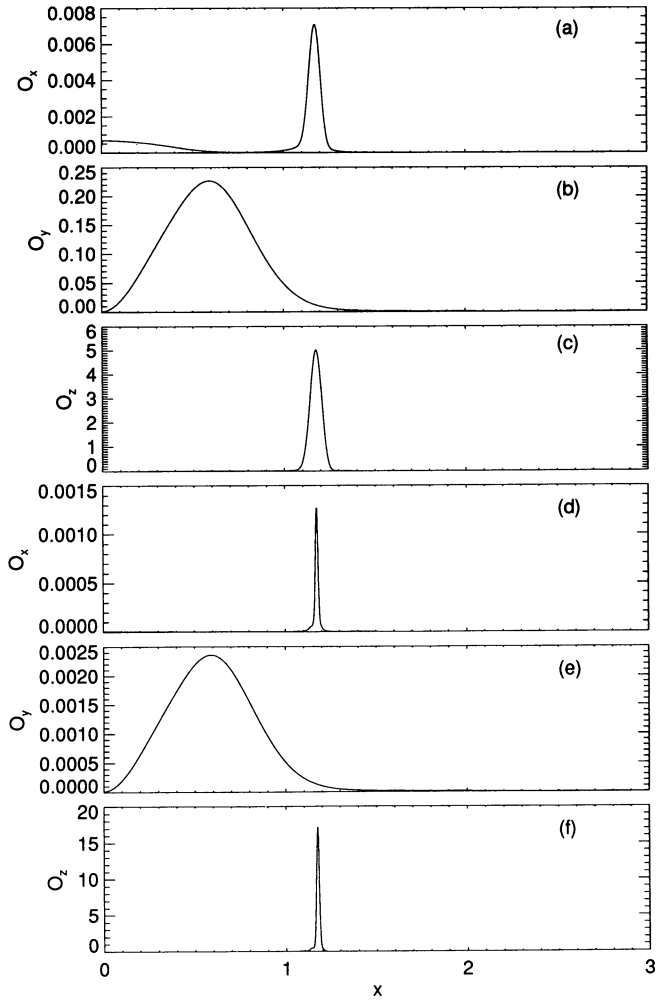

FIG. 8.—Spatial variation of the ohmic heating rates associated with each component of the current integrated over the interval $0 < t < 200$, $O_x = \int \eta j_x^2(x, t)dt$, etc. (*a*)–(*c*) employ $\eta = 10^{-4}$, while (*d*)–(*f*) have $\eta = 10^{-6}$.

we anticipate that the magnitude of the j_x heating ($\eta j_x^2 \propto \eta^{1/3}$) should be reduced by a factor of 4.6 from Figure 8*a* to Figure 8*d*, and this is close to the observed result of 5.5. The j_z heating peak in Figure 8*f* has also narrowed in x (by a factor of $\sim$4.2), while the magnitude of the peak has increased by $\sim$3.6. Thus the total dissipation by j_z (i.e., the area under the j_z heating plots in Fig. 8) is approximately independent of η—a familiar result from steady oscillatory linear theory. It is evident from Figure 8 that as η is reduced further (to realistic coronal values of order 10^{-12}) the only significant heating contribution will be from the field-aligned current at the Alfvén resonance.

The present experiment is time dependent and consequently not posed in a simple enough fashion to permit a straightforward derivation of universal scaling laws with η. Nonetheless, it is apparent from our results that steady state theory may provide a useful guide to predicting the amplitude and widths of resonances. Departures from the steady state scaling will be addressed later.

Figure 9 shows the variation of total ohmic heating within the cavity as a function of time for $\eta = 10^{-4}$ (Figs. 9*a*–9*c*) and $\eta = 10^{-6}$ (Figs. 9*d*–9*f*) [i.e., the quantities $P_x = \int_0^3 \eta j_x^2(x, t)dx$, etc.]. Once again, the heating from j_y is associated with the fast mode and has a peak-to-peak period of 1.2, which is half of the first fast eigenperiod ($2\pi/2.54 = 2.47$): This result is to be expected—if j_y is oscillatory and periodic over 2.47, then ηj_y^2 will be periodic over half this interval. That j_y is associated with the fast mode is reflected in the fact that the envelope of the j_y heating reproduces the behavior of the u_x envelope in Figure 6*a*—we would expect even closer correlation, with the envelope of u_x^2. Note that when η is reduced to 10^{-6} (Figs. 9*d*–9*f*) the j_y heating rate is reduced, scaling as η (Fig. 9*e*).

Now consider the heating from field-aligned currents, $j_z(P_z)$. The heating curves in Figures 9*c* and 9*f* are surprisingly free from oscillations at the resonant Alfvén period (2.47). (Note that the heating rates in Fig. 9 are integrated over x, but are *not* integrated or averaged in time in any manner.) When $\eta = 10^{-4}$ the variation of j_z heating (Fig. 9*c*) approximately follows the envelope of the j_y heating (Fig. 9*b*), but there appears to be a slight time delay. For example, j_y heating has a peak at $t = 69$, whereas j_z heating has a peak at $t = 78$. By comparing the

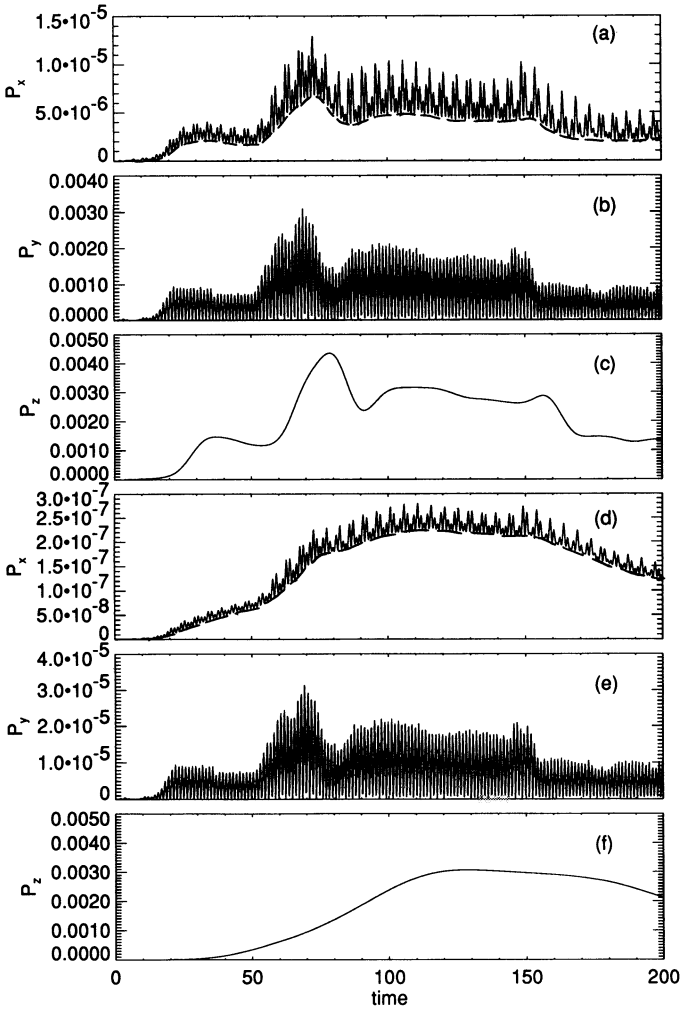

FIG. 9.—Temporal variation of the ohmic heating rates associated with each component of the current integrated over the range $0 < x < 3$, $P_x = \int \eta j_x^2(x, t)dx$, etc. (*a*)–(*c*) employ $\eta = 10^{-4}$, while (*d*)–(*f*) have $\eta = 10^{-6}$. The oscillations in the heating from j_x and j_y (P_x and P_y) are associated with the fast eigenmode oscillation. There are no such fluctuations in the heating produced by $j_z(P_z)$, which arises from the Alfvén wave. These heating rates have *not* been time averaged. The "offset" referred to in the text is indicated by a dashed line in (*a*) and (*d*).

times of several such features in these plots we estimate that the j_z features in Figure 9*c* appear ~ 10 time units after the feature has occurred in the j_y envelope (Fig. 9*b*). We return to this issue later. We also note that the effect of reducing η on the j_z heating is to produce a gradual rise in heating and to smooth out many of the features present when $\eta = 10^{-4}$ (cf. Figs. 9*c* and 9*f*). However, the magnitude of the heating appears to be independent of η.

It was noted from Figure 8 that j_x had contributions from both the fast and Alfvén modes. This is supported further by examining the j_x heating (P_x in Fig. 9*a*), which we shall divide into two components: The first (the "offset") may be defined by joining consecutive local minima together (Fig. 9*a*, *dashed line*). The second component is the oscillatory behavior above the offset level. The oscillations are associated with the fast mode and scale proportional to η (identical to the j_y heating). The offset of the j_x heating follows the general variation of the j_z, or Alfvénic, heating for both values of η. Further evidence that this offset arises from Alfvénic heating may be gained by considering the scaling with η: A steady state calculation gives the j_x heating integrated in x scaling as $\eta j_x^2 \Delta x \propto \eta^{2/3}$ (since $j_x \propto \eta^{-1/3}$ and $\Delta x \propto \eta^{1/3}$). Thus a steady state analysis suggests the offset in Figure 9*d* should be 22 times smaller than the offset in Figure 9*a*. It is difficult to choose a suitable time in our simulation for comparing the j_x heating offset because of the time-dependent nature of our calculation. However, the heating offsets in both runs are relatively constant over the interval $100 < t < 150$ and give reduction by a factor of 22—in surprisingly good agreement with the steady state scaling of 22.

5.5. *Optimal Coupling/Heating*

We have suggested that two criteria must be met if we are to couple boundary motions efficiently to Alfvén resonances. Moreover, since any energy deposited in Alfvén waves will ultimately be dissipated as ohmic heating, the heating rate may be used as a measure of the energy coupled into the resonance. This is particularly true for small η, where we have seen the heating comes almost exclusively from the Alfvén resonance. Thus we anticipate that the total ohmic dissipation will be a measure of the efficiency with which the boundary motions drive a resonance, and it is in this spirit that we employ $Q = \int \eta j^2 \, dx \, dt$ as a diagnostic. (We integrate over $0 < x < 3$ and $0 < t < 200$.)

Figures 10*a* and 10*b* display the energy dissipated as a function of k_z for $\eta = 10^{-4}$ and 10^{-6}, respectively. The results presented previously had $k_z = 1.23$, and these runs supplied the points in Figure 10 for this value of k_z. Identical experiments were performed for different k_z, and the plots in Figure 10 resulted. Apart from a slight difference in amplitude (discussed later) the plots are very similar. Perhaps the features over $0.7 < k_z < 0.9$ when $\eta = 10^{-4}$ are due to the fast mode, since these are absent in the $\eta = 10^{-6}$ results. Nevertheless, the two curves are very similar and appear to be exhibiting some asymptotic behavior as η is reduced. Since Figure 10*b* will be closer to any asymptotic results, we shall interpret this data set.

A clear rise in heating is observed for $k_z \approx 0.6$. This is because for $k_z \lesssim 0.6$ there is no global/fast eigenfrequency inside the Alfvén continuum (see Fig. 3). For $k_z \gtrsim 0.6$ one or more fast eigenfrequencies lie in the Alfvén continuum and are thus able to drive a resonance. Thus our second criterion explains the step in heating at $k_z \approx 0.6$.

Other features in Figure 10 include four strong heating spikes for $k_z = 1.075$, 1.16, 1.26, and 1.35. We have developed

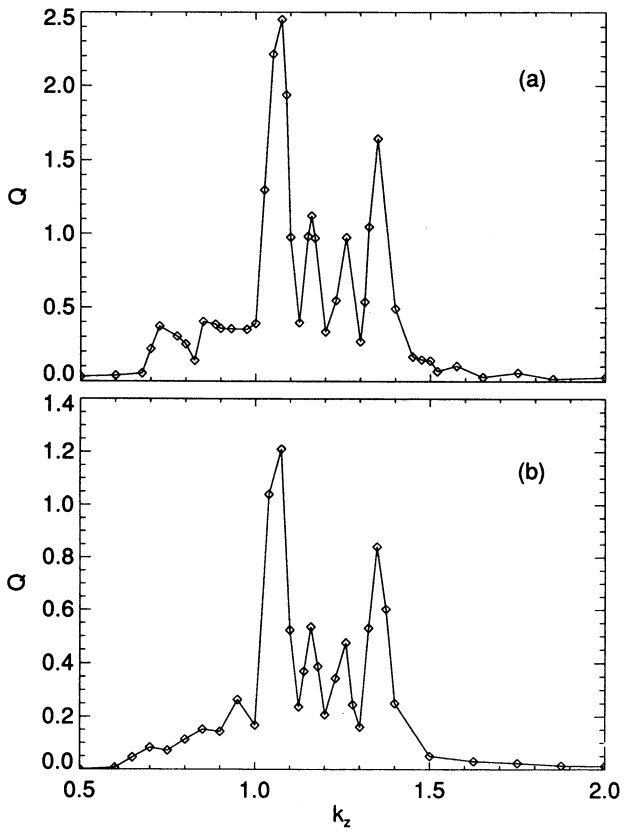

FIG. 10.—Total ohmic heating integrated over $0 < x < 3$ and $0 < t < 200$ ($Q = \int \eta j^2 \, dx \, dt$) for runs with varying k_z: (*a*) $\eta = 10^{-4}$ and (*b*) $\eta = 10^{-6}$. Significant energy is dissipated for a limited range of k_z (from 0.6 to 1.5).

the following ad hoc explanation of these peaks: Since the fundamental global/fast mode must be driving the resonances we may use Figure 4 to estimate its position. Knowing the position (and thus the Alfvén speed; Fig. 2) and k_z we may estimate the frequency of the Alfvén resonance. This procedure gives resonant positions of 1.22, 1.19, 1.17, and 1.14, while the resonant frequencies are 2.38, 2.49, 2.56, and 2.67, respectively. Figure 11 shows an enlargement of Figure 5*b*, the Fourier

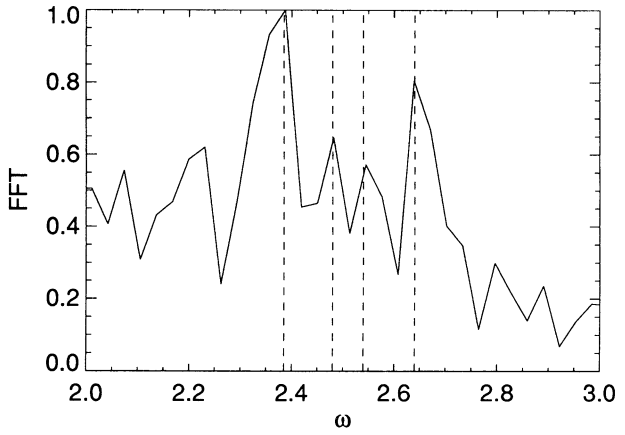

FIG. 11.—Enlargement of Fig. 5*b* (the FFT of the driving velocity) over the range $2 < \omega < 3$. The four peaks at 2.385, 2.48, 2.54, and 2.64 may be identified with the four heating peaks in Fig. 10.

transform of the boundary motion driving spectrum. We see that there are actually local peaks in the driving spectrum at frequencies 2.385, 2.48, 2.54, and 2.64 which correspond well with the k_z, or equivalently ω_A, peaks in heating rate. (Note that we have not determined the true location of the peaks in Fig. 10 very accurately.)

The small heating rates in Figure 10*b* above $k_z = 1.5$ may be understood by a similar analysis; $k_z = 1.5$ gives $x_r = 1.125$, so $V_A(x_r) = 1.855$ and $\omega_A(x_r) = 2.83$. We see from Figure 11 that this frequency is in the high-frequency tail of the driving spectrum and so is weakly driven. Indeed, $k_z = 1.5$ is the point above which our first criterion (namely, that the fast eigenfrequencies lie within the driving spectrum) is violated, consequently when $k > 1.5$ coupling is weak.

The criteria we propose if efficient coupling of boundary motions to Alfvén resonance is to be achieved give a window in k_z-space of $0.6 < k_z < 1.5$ in which we anticipate strong coupling may be realized. This is in excellent agreement with our numerical results.

6. DISCUSSION

We now consider some of the finer details of our time-dependent results. Ideal time-dependent resonant absorption studies by Mann, Wright, & Cally (1995) have shown how the resonance develops increasingly fine structure with time. They demonstrated how an important scale length across the resonance could be estimated reliably from the decoupled ($k_y = 0$) phase mixing length, L_{ph}. Taking a wavenumber in the z-direction and setting $\partial/\partial y = 0$, the governing equations (1) give a decoupled equation for u_y or b_y, the solution of which is

$$u_y \quad \text{or} \quad b_y = A(x) \exp\left[i\omega_A(x)t\right] . \tag{19}$$

Taking the derivative in x, and introducing a local wavenumber $k_x(x)$, gives

$$\frac{\partial b_y}{\partial x} = \frac{dA}{dx} \exp\left(i\omega_A t\right) + i\omega'_A t b_y \equiv ik_x(x) b_y , \tag{20}$$

where $\omega'_A = d\omega_A/dx$. For large times $k_x \approx \omega'_A t$, and the local scale length of perturbations in x is

$$L_{ph} = \frac{2\pi}{k_x} = \frac{2\pi}{\omega'_A t} . \tag{21}$$

This defines the phase mixing length, which decreases with time as neighboring field lines drift more and more out of phase.

Equation (21) can be inverted to give a phase mixing time (t_{ph}) by which we mean the time it takes for phase mixing to achieve a given scale L:

$$t_{ph} = \frac{2\pi}{\omega'_A L} . \tag{22}$$

In the coupled mode problem of § 5 ($k_y \neq 0$) we shall not have solutions of exactly the form in equation (19). Nevertheless, the time and spatial scales given in equations (21) and (22) still provide reliable estimates of these scales. We shall now use these notions to understand some of the features in our coupled results.

Recall that in Figures 9*b* and 9*c* we noted that the j_z (Alfvénic) heating curve was delayed relative to the j_y (fast) heating envelope by ~ 10 time units (§ 5.4). When $\eta = 10^{-4}$ the width of the Alfvénic energy density (Fig. 7*a*) and the Alfvénic spatial heating (j_z heating in Fig. 8*c*) suggest the resonance has scale length of ~ 0.074, corresponding to the length at which diffusion dominates convection (L_d). From a dynamic point of view we could argue that Alfvénic energy is initially excited with a scale length much greater than the diffusion length, and then phase mixing commences. For short times, when $L_d < L_{ph}$ there is little ohmic dissipation, and the Alfvén waves phase mix without loss of amplitude. However, by the time $L_{ph} = L_d$ for some Alfvénic component, its amplitude has been much reduced, and all its energy is essentially dissipated. The ohmic dissipation of these phase mixing Alfvén components will occur on scales $\gtrsim L_d$, and a length of $2L_d$ would be a reasonable "average" dissipation length. Thus we would anticipate that, once energy has been coupled into Alfvén waves, it will take a delay of order $t_{ph} = \pi/(\omega'_A L_d)$ for the Alfvén waves to phase-mix to a length at which ohmic dissipation occurs. For the results in Figures 9*b* and 9*c*, this suggests j_z heating should be delayed behind j_y heating by ~ 9 time units—in good agreement with the observed value.

Reducing η from 10^{-4} to 10^{-6} reduces the width (and dissipation length) by a factor of ~ 5. Thus we expect j_z heating in Figure 9*f* to be delayed by ~ 50 time units compared with j_y heating (Fig. 9*e*). It is difficult to corroborate this prediction as we only run up to $t = 200$. However, we do note that the peak j_y heating is at $t = 70$, while that of j_z is at $t = 120$, providing some support for our claim.

As η is reduced the energy resides in the Alfvén waves for longer times before being dissipated, since energy must cascade or phase-mix, to finer scales. It is this property, coupled with the fact that energy is really dissipated at varying rates on a range of scale lengths, that probably provides the averaging or smoothing effect when comparing the j_z heating in Figures 9*c* and 9*f* for $\eta = 10^{-4}$ and 10^{-6}, respectively.

The magnitude of the total energy dissipated when $\eta = 10^{-4}$ and 10^{-6} (see Fig. 10) changes by a factor of ~ 2. The difference can probably be attributed to the fact that for smaller η it takes longer for Alfvén waves to dissipate their energy—a fact supported by the very gradual rise in j_z (Alfvénic) heating when $\eta = 10^{-6}$ compared to 10^{-4} (Figs. 9*c* and 9*f*). The areas under these j_z heating curves are essentially the total heating (Fig. 10), and evidently the slow rise at early times produces a smaller total energy dissipation for smaller η.

It is interesting to note that Figures 3 and 4 predict that the first fast harmonic enters the Alfvén continuum when $k_z \approx 0.55$. Thus in Figure 10*b* the point $k_z = 0.6$ should contain an Alfvén resonance, yet it exhibits remarkably low heating. The reason for this may be understood by considering the positions of the resonances. For $k_z = 0.6$, 0.7, and 0.8, the Alfvén resonances occur at $x_r = 1.5$, 1.37, and 1.31, at which points $\omega'_A = 0.67$, 2.12, and 3.03. Note that ω'_A is much smaller for $k_z = 0.6$ and $x_r = 1.5$—due principally to the decreasing Alfvén speed gradient as x changes from 1.4 to 1.6 (see Fig. 2). Since $\omega'_A(x_r)$ is so small for $k_z = 0.6$ the phase mixing time for dissipation is very large (~ 260 time units), and given that we only run for 200 time units, there is very little dissipation. The phase mixing times to $2L_d$ for $k_z = 0.6$, 0.7, and 0.8 are 260, 84, and 60 time units, so for a flat driving spectrum we expect the total energy dissipation to increase with k_z over this limited range.

Recall the spatially integrated heating rates displayed as a function of time in Figures 9*c* and 9*f*. A remarkable property of this figure is the absence of fluctuations with a period similar to

that of the Alfvén resonance. To our knowledge the observation of a temporally steady Alfvénic heating rate has not been reported previously—perhaps because most studies time-average the heating in some fashion.

In an effort to study the steady Alfvénic heating we drove our boundary with a harmonic motion of period 2.64, which corresponds to the first fast eigenperiod as we set $k_z = 1.075$ for this run ($x_r = 1.21$). After $t = 600$ the transient disturbances have been dissipated ($\eta = 10^{-4}$) and our solution essentially has a time dependence of exp ($i2\pi t/2.64$). The ohmic dissipation should be periodic over half the driving period (i.e., 1.32), and Figures 12*a*–12*e* show $R_z = \eta j_z^2(x, t)$ for times 0.0, 0.33, 0.66, 0.99, and 1.32, respectively, following $t = 600$. We see that there are waves of current density (or ohmic heating) propagating across the resonance. The heating peaks have been labeled 1, 2, and 3. Following their time development we see that these peaks begin at large x, where they are very small. As the peak moves to the center of the resonance it grows and thereafter moves to smaller x and diminishes in size. (Note that Steinolfson & Davila's Figure 7 shows three heating spikes and has a phase somewhere between our Figs. 12*b* and 12*c*). These heating spikes evidently have the property that the area under them at *any* time is constant. This may have implications for signatures of heating in the corona.

On grounds of current continuity we expect $j_x \propto \int j_z\, dx$, and so the Alfvénic j_x heating should have two peaks in x. Once again, $\int \eta j_x\, dx$ integrated across the resonance appears to be independent of time.

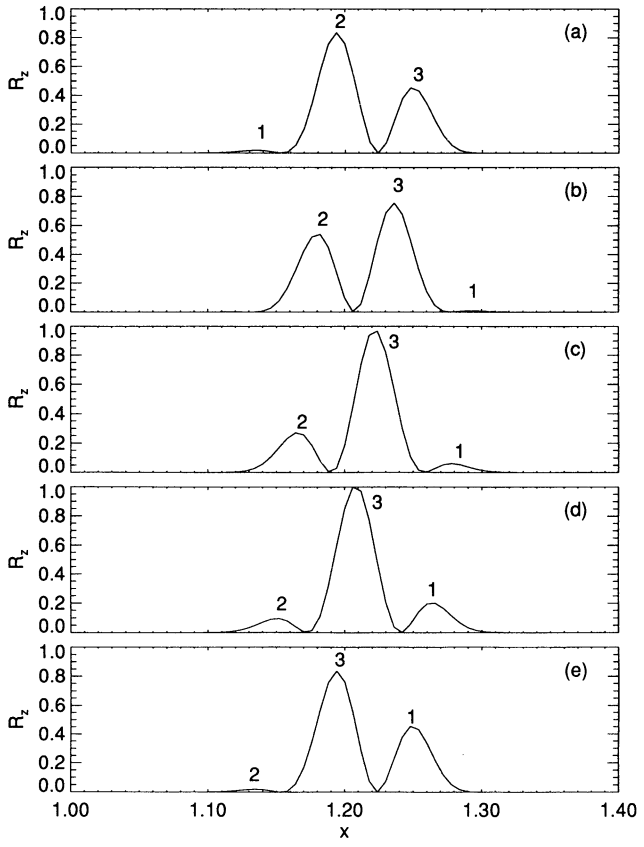

FIG. 12.—Spatial variation of the j_z ohmic dissipation [$R_z = \eta j_z^2(x, t)$] across the Alfvén resonance for a cavity that has been driven harmonically with a period 2.64 ($\eta = 10^{-4}$). By $t = 600$ transients had died away, and all perturbations oscillated with the driving period. The panels display snapshots of the ohmic heating at times (*a*) 0.0, (*b*) 0.33, (*c*) 0.66, (*d*) 0.99, and (*e*) 1.32, subsequent to $t = 600$, and thus cover one cycle of the heating perturbations.

7. CONCLUSIONS

In this paper we have considered the time-dependent coupling of broadband frequency boundary motions to Alfvén resonances—a problem relevant to geomagnetic pulsations and coronal heating. We find two criteria must be met for efficient coupling. First, the global or fast eigenfrequencies of the MHD cavity must lie within the frequency spectrum of the driving motions. (This ensures that a relatively large amplitude fast mode will be excited within the cavity.) Second, the fast eigenfrequency must also lie within the Alfvén continuum. When these conditions are satisfied the broadband driving source is effectively "filtered" by the cavity, producing disturbances in the cavity that are essentially a superposition of fast eigenmodes. Each of these modes oscillates with its own natural frequency and provides a coherent driver suitable for establishing an Alfvén resonance (cf. Kivelson & Southwood 1985 for the undriven case).

Boundary motions readily excite fast eigenmodes within a few periods, where they subsequently store energy. Transient boundary motions simply add more energy to the cavity where the fast modes do not exhibit transient behavior: In the absence of dissipation the amplitude of the fast mode will be related to the time-integrated Poynting flux normal to the boundary—thus discontinuities in Poynting flux do not produce discontinuities in fast-mode amplitude. The steady accumulation of fast-mode energy can be seen in Figure 6*a*. The fast-mode amplitude within the cavity is so free from transients that it acts as a quasi-steady driver of Alfvén resonances; we have found that the steady state scaling laws (with η) provide a remarkably good description of the resonance.

For smaller η it takes longer for the ohmic heating at the resonance to grow, and we can explain this in terms of the phase mixing time—the time it takes Alfvén waves to develop fine enough structure (i.e., large enough field-aligned currents) to dissipate energy. We expect this time to scale as $\eta^{1/3}$. We have also given a physical interpretation to the importance of fast or global modes for efficient coupling to resonances noted in previous studies. The fast/global mode acts as an intermediary that communicates the boundary motion's energy to the location of the Alfvén resonance. In fact, we could view the whole process as two resonances: the first is the resonant excitation of a fast eigenmode by boundary motions; the second is the Alfvén resonance driven by the fast eigenmode.

In future studies we shall apply the ideas developed in this paper to resonance problems in magnetospheric and solar theory. For example, it seems evident that the Kelvin-Helmholtz instability which has been invoked at the magnetopause in order to supply a steady harmonic driver of geomagnetic pulsations is not essential: General, time-dependent disturbances of the magnetopause can be filtered by the magnetospheric cavity and thus produce a suitable driver of pulsations. Coronal heating by resonant coupling to Alfvén waves should be possible on closed field line structures that are driven by quite random footpoint, or boundary, motions. Once again the arcade or flux tube will filter the driving spectrum to produce a fast-mode disturbance that will be suitable for establishing Alfvén resonances.

This work was carried out while A. N. W. was supported by a UK PPARC Advanced Fellowship.

REFERENCES

Allan, W., Poulter, E. M., & White, S. P. 1986a, Planet. Space Sci., 34, 1189
Allan, W., White, S. P., & Poulter, E. M. 1986b, Planet. Space Sci., 34, 371
Budden, K. G. 1961, Radio Waves in the Ionosphere (London: Cambridge Univ. Press)
Cally, P. S. 1991, J. Plasma Phys., 45, 453
Chen, L., & Cowley, S. C. 1989, Geophys. Res. Lett., 16, 895
Chen, L., & Hasegawa, A. 1974, J. Geophys. Res., 79, 1024
Dungey, J. W. 1954, Electrodynamics of the Outer Atmosphere (Sci. Rep. 69) (University Park: Pennsylvania State Univ.)
———. 1967, in Physics of Geomagnetic Phenomena, Vol. 2, ed. S. Matsushita & W. H. Campbell (San Diego: Academic), 913
Goedbloed, J. P. 1975, Phys. Fluids, 18, 1258
Goossens, M., & Hollweg, J. V. 1993, Solar Phys., 145, 19
Grossmann, W., & Smith, R. A. 1988, ApJ, 332, 476
Hollweg, J. V. 1984, ApJ, 227, 392
———. 1987, ApJ, 320, 875
———. 1990, Planet. Space Sci., 38, 1017
Inhester, B. 1986, J. Geophys. Res., 91, 1509
———. 1987, J. Geophys. Res., 92, 4751
Ionson, J. A. 1978, ApJ, 226, 650
Kivelson, M. G., & Southwood, D. J. 1985, Geophys. Res. Lett., 12, 49
———. 1986, J. Geophys. Res., 91, 4345
Lee, D. H., & Lysak, R. L. 1989, J. Geophys. Res., 94, 17,097
———. 1991. J. Geophys. Res., 96, 3479
Lee, M. A., & Roberts, B. 1986, ApJ, 301, 430
Lin, N., Engebretson, M. J., Reinleitner, L. A., Olson, J. V., Gallagher, D. L., Cahill, Jr., L. J., Slavin, J. A., & Persoon, A. M. 1992, J. Geophys. Res., 97, 14, 859
Mann, I. R., Wright, A. N., & Cally, P. S. 1995, J. Geophys. Res., submitted
Mond, M., Hameiri, E., & Hu, P. N. 1990, J. Geophys. Res., 95, 89
Poedts, S., & Goossens, M. 1991, Solar Phys., 133, 281
Poedts, S., Goossens, M., & Kerner, W. 1989, Solar Phys., 23, 83
———. 1990a, Comput. Phys. Comm., 59, 75
———. 1990b, Comput. Phys. Comm., 59, 95
Poedts, S., Kerner, W., & Goosens, M. 1989, J. Plasma Phys., 42, 27
Radoski, H. R. 1974, J. Geophys. Res., 79, 595
———. 1976, Environmental Res. Paper 559 (Hanscom AFB, MA: AFGL)
Rae, I. C., & Roberts, B. 1981, Geophys. Astrophys. Fluid Dyn., 18, 197
Rickard, G. J., & Wright, A. N. 1994, J. Geophys. Res., 99, 13,455
Sakurai, T., Goossens, M., & Hollweg, J. V. 1991a, Solar Phys., 133, 227
———. 1991b, Solar Phys., 133, 247
Sedlacek, Z. 1971, J. Plasma Phys., 5, 239
Southwood, D. J. 1974, Planet. Space Sci., 22, 483
Southwood, D. J., & Kivelson, M. G. 1986, J. Geophys. Res., 91, 6871
———. 1990, J. Geophys. Res., 95, 2301
Steinolfson, R. S., & Davila, J. M. 1993, ApJ, 415, 354
Thompson, M. J., & Wright, A. N. 1993, J. Geophys. Res., 98, 15, 551
Vaclavik, J., & Appert, K. 1991, Nucl. Fusion, 31, 1945
Wright, A. N. 1991, Geophys. Res. Lett., 18, 1951
———. 1992a, J. Geophys. Res., 97, 6439
———. 1992b, J. Geophys. Res., 97, 6429
———. 1994, in Physical Signatures of Magnetospheric Boundary Layer Processes, ed. J. A. Holtet & A. Egeland (Dordrecht: Kluwer), 329
Wright, A. N., & Thompson, M. J. 1994, Phys. Plasmas, 1, 691
Zalesak, S. T. 1979, J. Comput. Phys., 31, 335
Zhu, X., & Kivelson, M. G. 1988, J. Geophys. Res., 93, 8602